Strain Is More Important Than Electrostatic Interaction in Controlling the pK_a of the Catalytic Group in Aspartate Aminotransferase[†,||]

Hiroyuki Mizuguchi,[‡] Hideyuki Hayashi,[‡] Kengo Okada,[§] Ikuko Miyahara,[§] Ken Hirotsu,[§] and Hiroyuki Kagamiyama*[,‡]

Department of Biochemistry, Osaka Medical College, Takatsuki 569-8686, Japan, and Department of Chemistry, Osaka City University, Osaka 558-8585, Japan

Received June 20, 2000; Revised Manuscript Received October 25, 2000

ABSTRACT: Systematic single and multiple replacement studies have been applied to *Escherichia coli* aspartate aminotransferase to probe the electrostatic effect of the two substrate-binding arginine residues, Arg292 and Arg386, and the structural effect of the pyridoxal 5′-phosphate-Asn194−Arg386 hydrogen-bond linkage system (PLP-N-R) on the pK_a value of the Schiff base formed between pyridoxal 5′-phosphate (PLP) and Lys258. The electrostatic effects of the two arginine residues cannot be assessed by simple mutational studies of the residues. PLP-N-R lowers the pK_a value of the PLP−Lys258 Schiff base by keeping it in the distorted conformation, which is unfavorable for protonation. Mutation of Arg386 eliminates its hydrogen bond with Asn194 and partially disrupts PLP-N-R, thereby relaxing the strain of the Schiff base. On the other hand, mutation of Arg292, the large domain residue that interacts with the small domain residue Asp15, makes the domain opening easier. Because PLP-N-R lies between the two domains, the domain opening increases the strain of the Schiff base. Therefore, the true electrostatic effects of Arg292 and Arg386 could be derived from mutational analysis of the enzyme in which PLP-N-R had been completely disrupted by the Asn194Ala mutation. Through the analyses, we could dissect the electrostatic and structural effects of the arginine mutations on the Schiff base pK_a. The positive charges of the two arginine residues and the PLP-N-R-mediated strain of the Schiff base lower the Schiff base pK_a by 0.7 and 1.7, respectively. Thus, the electrostatic effect of the arginine residues is not as strong as has historically been thought, and this finding substantiates our recent finding that the imine-pyridine torsion of the Schiff base is the primary determinant (2.8 unit decrease) of the extremely low pK_a value of the Schiff base [Hayashi, H., Mizuguchi, H., and Kagamiyama, H. (1998) *Biochemistry 37*, 15076−15085].

Aspartate aminotransferase (aspartate:2-oxoglutarate aminotransferase, EC 2.6.1.1; AspAT)[1] catalyzes reversible transamination reactions between dicarboxylic amino and keto acids, in which the amino group temporarily resides on the coenzyme pyridoxal 5′-phosphate (PLP) to form pyridoxamine 5′-phosphate (PMP) (eqs 1 and 2):

$$\text{aspartate} + E_L \rightleftarrows \text{oxalacetate} + E_M \quad (1)$$

$$\text{2-oxoglutarate} + E_M \rightleftarrows \text{glutamate} + E_L \quad (2)$$

Here, E_L and E_M denote the PLP form and the PMP form of the enzyme, respectively.

The enzyme from various sources has been extensively studied, and the mechanism of action has been proposed from X-ray crystallographic and enzymological studies (*2*−*12*). In the active site, Lys258[2] forms a Schiff base with the coenzyme PLP. Arg386 and Arg292* are the anchoring sites for the α- and ω-carboxylate groups, respectively, of dicarboxylic substrates (*13*−*15*; Figure 1). The pK_a of the imine N of the PLP−Lys258 Schiff base has a strikingly low value of 6.5−6.8, compared to the value of around 10 of PLP Schiff bases (with the pyridine N protonated) in aqueous solutions (*16*).[3] On binding of substrate dicarboxylic amino acids, the pK_a of the imine N is increased, and a proton is transferred from the α-ammonium (protonated amino)

[†] This work was supported by the "Research for the Future" Program (Project JSPS-RFTF96L00506 to H.K.) and the Grant-in-Aid for Scientific Research (00183913 to H.H.) of the Japan Society for the Promotion of Science, and the SUNBOR Grant (to H.H.) from the Suntory Institute for Bioorganic Research.

[||] Coordinates for the mutant AspAT have been deposited in the RSCB Protein Data Bank as entries 1G4V (N194A/Y225F), 1G4X (N194A/R292L), 1G7W (N194A/R386L), and 1G7X (N194A/R292L/R386L).

* To whom correspondence should be addressed. Fax: +81-726-84-6516. E-mail: med001@art.osaka-med.ac.jp.

[‡] Osaka Medical College.

[§] Osaka City University.

[1] Abbreviations: AspAT, aspartate aminotransferase; PLP, pyridoxal 5′-phosphate; PMP, pyridoxamine 5′-phosphate; PLP-N-R, pyridoxal 5′-phosphate-Asn194-Arg386 hydrogen-bond linkage system; HEPES, *N*-(2-hydroxyethyl)piperazine-*N*′-(2-ethanesulfonic acid); MES, 2-(*N*-morpholino)-ethanesulfonic acid; TAPS, *N*-Tris(hydroxymethyl)methyl-3-aminopropanesulfonic acid; ΔpK_a, change in the Schiff base pK_a upon mutation.

[2] The amino acid residue is numbered according to the sequence of pig cytosolic aspartate aminotransferase (*1*). An asterisk indicates that the residue comes from the neighboring subunit. R386L AspAT denotes the mutant aspartate aminotransferase in which the residue Arg386 was replaced by a leucine residue. The other mutant enzymes are expressed in the same way.

10.1021/bi001403e CCC: $20.00
Published on Web 12/15/2000

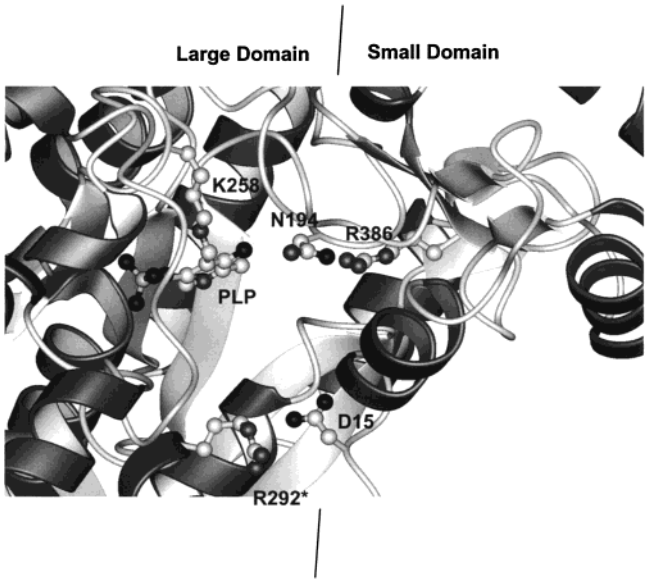

FIGURE 1: Active site of AspAT shown in the ribbon model. The residues discussed in this study, Lys258, Asn194, Arg386, Arg292*, Asp15, and PLP, are shown in the ball-and-stick model (white, carbon; black, oxygen; gray, nitrogen). The residues Arg386 and Asp15 are located in the small domain. Asn194 resides in the loop protruding from the large domain. Hydrogen bonds are formed between O3′ of PLP and Nδ of Asn194, and between Oδ of Asn194 and Nη of Arg386. This figure and the following molecular graphics are drawn using MOLMOL (*29*).

group of the substrate to the imine N. The resultant free amino group undergoes a nucleophilic attack on the imine, which has increased its electrophilicity by protonation, to form the PLP-substrate Schiff base. This step is called transaldimination reaction (Scheme 1). The increase in the Schiff base pK_a is estimated to be around 2.0 by comparing the pK_a values between the unliganded enzyme and maleate- or succinate-bound enzymes (*17*, *20*), and this is the marginal value required for the transaldimination reaction not to be rate determining in the catalytic process (*12*). In the classical mechanism to explain this, Ivanov and Karpeisky (*21*) proposed that the pK_a of the PLP−Lys258 Schiff base in the unliganded enzyme is lowered by electrostatic interaction with the positive charges of Arg386 and Arg292* and that neutralization of the two charges on binding of the dicarboxylic substrates increases the pK_a.

Recently, however, we have shown that the imine−pyridine torsion angle of the PLP−Lys258 Schiff base greatly lowers its pK_a and is crucial for the successive increase in the pK_a during catalysis (*12*). Therefore, the role of the electrostatic interaction between the arginine residues and the PLP−Lys258 Schiff base in the modulation of the Schiff base pK_a needs to be reinvestigated. Because the torsion of the PLP−Lys258 Schiff base is largely maintained by the hydrogen-bond linkage system including the guanidinium group of Arg386, the amide group of Asn194, and the phenolic O3′ of PLP (*4*−*8*), Arg386 is considered to have both direct electrostatic and the Asn194-mediated *structural* effects on the pK_a of the Schiff base. To dissect these effects, we performed systematic mutational analysis on the two arginine residues and Asn194. The results were interpreted on the basis of the structural data of the mutant enzymes.

[3] Martinez-Carrion's group (*18*) has reported an unusually low pK_a value for the ϵ-amino group of Lys258 in the apoenzyme (8.0 compared to 10.5 in aqueous solutions). This may reflect the electrostatic environment of the active site of AspAT. However, as their study used apoenzyme instead of holoenzyme and the pK_a value is not that of the Schiff base, their results cannot be directly compared with our results.

EXPERIMENTAL PROCEDURES

Chemicals. MES and HEPES were from Dojin Laboratories (Kumamoto, Japan). *Escherichia coli* AspAT was obtained as previously described using the pUC19-*aspC* expression system (*13*, *22*). Site-directed mutagenesis of the *aspC* gene was performed on the single-stranded M13 mp18 phage, into which the gene was subcloned, using the oligonucleotide-directed in vitro mutagenesis system (ver. 2.1, Amersham, U.K.). The primers used to induce mutations were 5′-GCG-GCG-ATT-CTC-GCT-AAC-TAC-TC-3′ for R292L, and 5′-TTT-GCG-GTT-GCT-AGC-GGT-CTG-GTA-AAT-GTG-GCC-3′ for R386L. The mutant *aspC* genes were ligated back to pUC19. The N194A mutant plasmid was prepared as described previously (*20*). The double mutant R292L/R386L *aspC* gene was made from the R386L *aspC* gene using the R292L mutagenesis primer. Plasmids for other double and triple mutants were constructed by recombination of the single and R292L/R386L mutant plasmids using the restriction site *Eco*T22I located between the Asn194 and Arg292 codons. The expression of the wild-type and mutant *aspC* genes in AspAT-deficient *E. coli* cells and purification of the enzymes were performed as described previously (*13*, *22*).

Spectroscopic Analysis. Absorption spectra were measured using a Hitachi U-3300 spectrophotometer at 298 K. The buffer solution contained 50 mM buffer component(s) and 0.1 M KCl. The buffer components used were MES−NaOH, HEPES−NaOH, and TAPS−NaOH. Protein concentrations were generally $1-2 \times 10^{-5}$ M in subunit. The concentration of the AspAT subunit in solution was determined spectrophotometrically. The apparent molar extinction coefficients used were $\epsilon_M = 4.7 \times 10^4$ M^{-1} cm^{-1} for the PLP-form enzyme (*22*).

Crystallography. All mutant AspATs were subjected to crystallization by the hanging drop vapor diffusion method. A 10-μL drop containing 40−60 mg mL^{-1} protein, 10 mM potassium phosphate (pH 7.0), 10 μM PLP, and 0.3 mM NaN_3 was added to 10 μL of reservoir solution containing 10 mM potassium phosphate (pH 7.0), 10 μM PLP, 0.3 mM NaN_3, and 40% saturated ammonium sulfate, and equilibrated against 1 mL of reservoir solution at 293 K. After 4−7 days, the drop was seeded with a small crystal of wild-type AspAT obtained previously. Crystals with a size suitable (about 1.0 × 0.8 × 0.4 mm) for X-ray experiments were grown for 10−20 days for N194A/R292L, N194A/R386L, and N194A/R292L/R386L. Although the crystal of N194A was not obtained, N194A/Y225F used for another study formed a good crystal sufficient for analysis, and this was used as a model of N194A in the discussion. All mutant AspAT crystals are isomorphous with that of the wild-type AspAT. The diffraction data for N194A/Y225F were collected at the BL6A station of the photon factory, KEK, Tsukuba, Japan, using an X-ray beam of wavelength 1.00 Å at 293 K and Fuji imaging plates with a screenless Weissenberg camera for macromolecular crystallography (*23*). Data collection was performed using two crystals. The data were processed by

Scheme 1: Reaction of the PLP Form of AspAT with Aspartate Leading to the External Aldimine (*12*)[a]

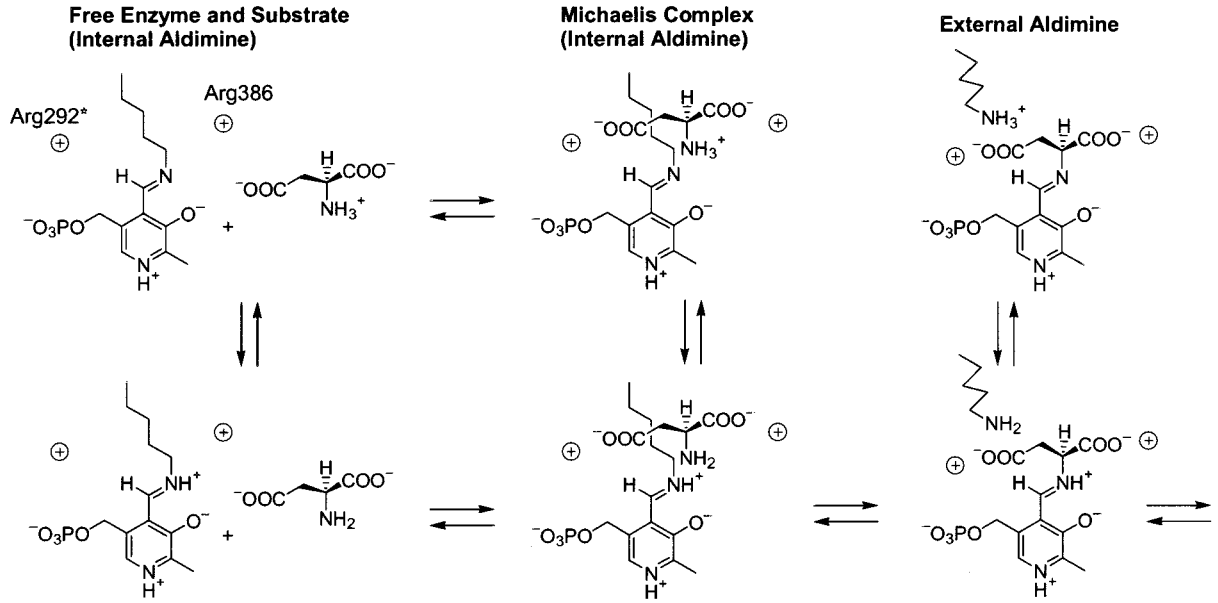

[a] The pK_a of the internal aldimine (Schiff base) of the free enzyme is 6.8. In the Michaelis complex, the pK_a of the internal aldimine is elevated to 8.8, whereas that of the α-amino group of aspartate is decreased from 9.6 to around 9. Therefore, the K_{eq} value for the interconversion between the two structures within the Michaelis complex is near unity. Because the intrinsic rate constant for the transaldimination reaction is about 3000 s^{-1}, the net transaldimination rate constant is calculated to be $3000 \times 1/(1 + 10^{9-8.8}) = 1200\ s^{-1}$ and is not rate-determining in the entire half reaction (apparent rate constant of 550 s^{-1}). After the formation of the external aldimine, the reaction proceeds via the quinonoid intermediate to the ketimine, which is hydrolyzed to form the PMP form of the enzyme and oxalacetate. See ref *12* for details.

Table 1: Data Collection, Crystal Data, and Refinement Statistics

	Data Collection			
crystal	N194A/ Y225F	N194A/ R292L	N194A/ R386L	N194A/ R292L/ R386L
cell parameters (Å)				
A	155.3	155.0	154.9	155.4
B	87.1	88.7	89.3	89.3
C	79.4	80.1	80.0	79.9
resolution limit (Å)	2.10	2.14	2.2	2.06
no. of reflections	92 716	144 708	127 902	101 587
no. of unique reflections	27 638	34 702	28 775	30 457
completeness (%)	91.0	90.1	93.5	96.2
R_{merge} (%)	6.7	6.5	6.7	8.7
	Refinement			
R factor (%)	20.9	22.9	21.7	22.9
resolution range (Å)	10−2.0	10−2.2	10−2.2	10−2.2
no. of solvent	215	169	213	244
temp. factor of protein (Å^2)	21.8	24.4	23.9	22.3
temp. factor of solvent (Å^2)	37.8	45.3	46.7	50.5
rmsd of bond distance (Å)	0.013	0.010	0.012	0.011
rmsd of bond angles (deg)	1.827	2.748	2.830	2.907

the program WEIS (*24*), COMBINE, and SCALE on HITAC M660K. The diffraction data of N194A/R292L, N194A/R386L, and N194A/R292L/R386L were collected with a Rigaku R-AXIS IIc image plate detector mounted on a Rigaku RU-200 rotating anode generator operated at 40 kV and 100 mA with monochromatized CuK_α radiation at room temperature. Each data collection was performed using one crystal. The diffraction data were processed with the R-AXIS software (T. Higashi, Rigaku, Akishima, Japan). The conditions for data collection are summarized in Table 1. Each of the four mutant AspAT structures was refined using the wild-type AspAT structure (PDB entry 1ARS) as the starting model. Model building and refinement were performed TOM/FRODO (*25*) and X-PLOR (*26*), respectively. The mutated residues and solvent molecules were modeled on the basis of $2|F_o| - |F_c|$ and $|F_o| - |F_c|$ electron density maps. The solvent molecules whose thermal factors were above 100.0 Å^2 after refinement were removed from the model. The quality of the model for each structure was evaluated using PROCHECK (*27*). Ramachandran plots in four mutant AspATs showed all the main chain atoms except Ser296 within the allowed region as observed in the wild-type AspATs (*8*). On the basis of electron density maps, it is confirmed that the conformation of Ser296 is correct. Table 1 contains a summary of the refinement statistics.

Estimation of the Electrostatic Effects of the Charged Groups on the Schiff Base. The Coulombic interaction energy (*E*) between the protonated Schiff base N and the charged groups other than the side chains of Arg292* and Arg386 of AspAT was estimated using the following equation of electrostatic potential energy:

$$E = \sum_i \frac{Z_i e_a^{\,2}}{4\pi\bar{\epsilon}\epsilon_0 r_i} \qquad (3)$$

where Z_i is the charge, r_i the distance between the charge and the Schiff base nitrogen, e_a the elementary charge, ϵ_0 the dielectric constant, and $\bar{\epsilon}$ the relative dielectric constant. The charge and the center of the charge of the respective groups were set as follows (in parentheses): arginine residue (+1, Cζ), lysine residue (+1, Nζ), aspartic acid residue (−1, Cγ), glutamic acid residue (−1, Cδ), N-terminal amino group (+1, N), C-terminal carboxylic group (−1, C), and PLP phosphate group (−2, P). Histidine residues were assumed to have no charges. Arg292* and Arg386 were omitted from the calculation. The value of $\bar{\epsilon}$ was set to be equal to the value expressed in Å of r_i (*28*). The effect of the change in

the electrostatic potential energy ΔE was related to the change in the Schiff base pK_a as follows:

$$\Delta E = -2.303RT\Delta pK_a \quad (4)$$

RESULTS AND DISCUSSION

pK_a of the PLP Schiff Base. The spectra of the PLP form of the mutant AspATs have absorption bands at around 360 nm, which is prominent at high pH, and at around 430 nm, which is prominent at low pH. These absorption bands are essentially identical to those of the wild-type enzyme (*2*, *9*−*12*), resulting from the unprotonated and protonated form, respectively, of the PLP−Lys258 Schiff base (Chart 1). The apparent molar absorption coefficients of the 430-nm absorption band were plotted against pH (Figure 2). The pK_a of the PLP−Lys258 Schiff base was obtained by fitting the plots to eq 5:

$$\epsilon_{app} = \epsilon_E + \frac{\epsilon_{EH} - \epsilon_E}{1 + 10^{pH-pK_a}} \quad (5)$$

ϵ_{EH} and ϵ_E denote the molar absorption coefficients of the Schiff-base-protonated and unprotonated enzymes, respectively, and pK_a denotes that of the imine N of the Schiff base. Some of the mutant enzymes, mostly those enzymes with N194A mutation, showed elevated basicity of the Schiff base, and hence their pK_a values were difficult to determine if the ϵ_E value was allowed to float during curve fitting. In such cases, we assumed that the ϵ_E value at 430 nm is equal to zero. This is a reasonable assumption, because the unprotonated PLP Schiff base does not show absorption at over 400 nm (*16*). The obtained pK_a values are summarized in Table 2.

Effects of Mutations of Arg292 and Arg386 on the PLP-Lys258 Schiff Base pK_a.* The pK_a values of R292L AspAT and R386L AspAT are higher than that of the wild-type AspAT by 0.14 and 0.46, respectively. The guanidinium group of Arg386 is closer to the Schiff base than that of Arg292* (9.8 Å compared to 14.5 Å; the values are the distances between the guanidinium Cζ of the arginine residues and Nζ of Lys258). Therefore, the difference in ΔpK_a may be considered to reflect closer electrostatic coupling of Arg386 and the Schiff base. However, the ΔpK_a of the R292L/R386L double mutation was 0.92; the value was 0.32 higher than the value expected from simple addition of ΔpK_a of the respective mutations (0.14 + 0.46 = 0.60). This indicates that the R292L and R386L mutations are not independent and that there are factor(s) other than electrostatic interaction that links the two arginine residues and the Schiff base.

PLP−Asn194−Arg386 Linkage and the Schiff Base pK_a. Asn194 exists between Arg386 and PLP, with its amide O and N hydrogen bonded to the guanidinium N of Arg386 and O3′ of PLP, respectively (Figure 1). Due to this hydrogen-bond linkage system (PLP-N-R), O3′ is pulled toward Asn194 and Arg386, while the imine bond of the Schiff base is pointed toward the opposite direction because it is tethered to the side chain of Lys258. As the result, the imine bond is out of the plane of the pyridine ring. Because the protonated Schiff base favors the coplanar orientation of the pyridine ring and the imine bond, PLP-N-R is considered to destabilize the protonated Schiff base, hence decreasing its pK_a value (ref *12*; Chart 1). The crystal structure of the R386F mutant enzyme showed that the side chain of Asn194 rotates by 25° around its Cβ−Cγ axis compared to the wild-type enzyme, due to the loss of the hydrogen bond between the side chains of Arg386 and Asn194 (*29*). Consequently, the hydrogen bond between Nδ of Asn194 and O3′ of PLP is weakened, and O3′ is moved

Chart 1: Structures of the PLP-Lys258 Schiff Bases Unprotonated (left) and Protonated (right) at the Imine N[a]

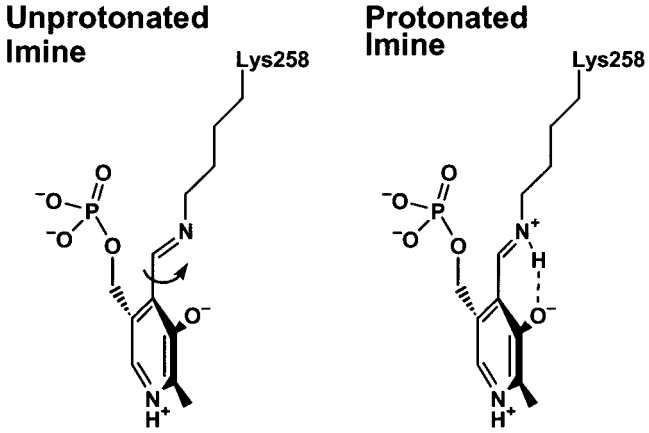

[a] In the planar structure, the imine bond and the pyridine ring reside in the same plane, and this structure is preferable for protonation of the imine N.

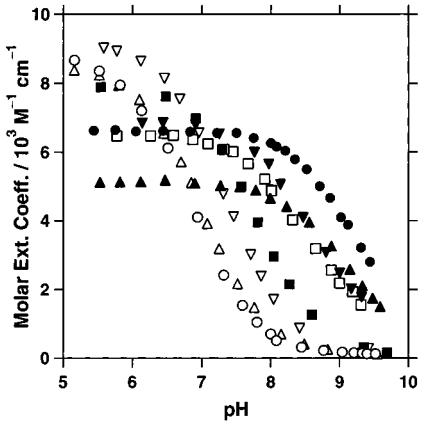

FIGURE 2: pH dependence of the apparent molar extinction coefficients at 430 nm of the wild-type and mutant AspATs at 298 K in the presence of 50 mM buffer component(s) and 0.1 M KCl. Open circles, wild type; open triangles, R292L; open reversed triangles, R386L; open squares, N194A; closed triangles, N194A/R292L; closed reversed triangles N194A/R386L; closed squares, R292L/R386L; closed circles, N194A/R292L/R386L.

Table 2: Aldimine pK_a Values of the Wild-Type and Mutant AspATs at 298 K[a]

enzyme	pK_a
wild-type	6.87 ± 0.01
R292L	7.01 ± 0.01
R386L	7.33 ± 0.01
R292L/R386L	7.79 ± 0.01
N194A	8.55 ± 0.03
N194A/R292L	9.10 ± 0.02
N194A/R386L	8.67 ± 0.03
N194A/R292L/R386L	9.22 ± 0.04

[a] The pK_a values of the internal aldimine of the wild-type and mutant AspATs were determined by fitting the apparent molar extinction coefficient of the enzymes at 430 nm to eq 5. The values are expressed as mean ± SD.

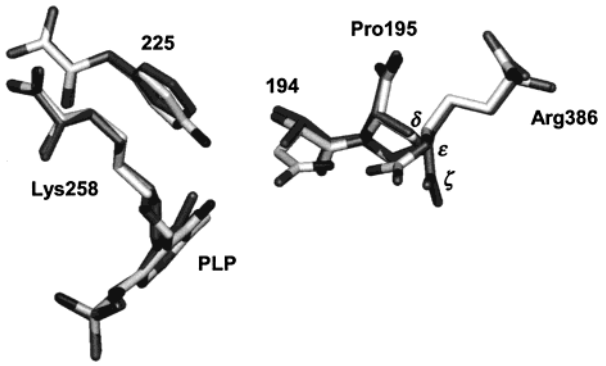

FIGURE 3: Superimposed structures of the active site residues of the wild-type and N194A/Y225F AspATs. The residues of N194A/Y225F AspAT are expressed in gray.

by 0.76 Å to the *si* face of the Schiff base, relaxing the torsion angle around C4−C4′ (*29*). Although the pK_a of this enzyme has not been determined, this observation strongly suggested that the Arg386 mutation has both direct electrostatic and indirect conformational (PLP-N-R-mediated) effects on the Schiff base pK_a. Therefore, we must take into account the involvement of PLP-N-R in discussing the effects of mutations on the two arginine residues. In this regard, we performed a systematic mutational analysis on Arg292*, Arg386, and Asn194.

Dissecting the Electrostatic and Conformational Contributions of the Arg386 Mutation to the Change in the Schiff Base pK_a. Because the conformational effect of the Arg386 mutation is mediated through the alteration of PLP-N-R, the electrostatic effect of Arg386 can be evaluated by analyzing the mutation in N194A AspAT, which lacks the entire system of PLP-N-R. For a discussion of the result, the position of Arg386 in N194A AspAT must be known, because the mutation of Asn194 may alter the side-chain conformation of the residues to which it forms hydrogen bonds. Unfortunately, however, the crystal structure of N194A AspAT has not been obtained. Therefore, we used the structure of N194A/Y225F AspAT as a substitute (Figure 3). Due to the loss of the hydrogen bond between Oδ of Asn194 and the guanidinium N of Arg386, the guanidinium group of Arg386 rotates by 70° around its Cδ−Nϵ axis, and Cζ, the center of charge, is moved by 1.3 Å to the solvent (Figure 3). As the result, the distance between Cζ of Arg386 and the imine N of the Schiff base changed only slightly from 9.8 to 10.6 Å. The R386L mutation of N194A AspAT showed a ΔpK_a of 0.12 (comparison of the pK_a values of N194A/R386L and N194A AspATs). Thus, out of the ΔpK_a = 0.46 on the R386L mutation of the wild-type AspAT, 0.12 is ascribed to the removal of the positive charge of Arg386 and the rest 0.34 to the alteration in PLP-N-R by disrupting the bond between Asn194 and Arg386.[4] The latter value was less than the value of 1.68 caused by N194A mutation. This may reflect that there still remains in R386L AspAT a hydrogen bond between O3′ of PLP and Asn194, and therefore, the strain of the Schiff base is less relaxed compared to that in N194A AspAT, the mutant enzyme that has lost the entire system of PLP-N-R.[5]

Domain Movements on Mutations. The N194A mutation did not significantly change the conformation of the protein backbone (as judged from the structure of N194A/Y225F AspAT). However, because this mutation removed PLP-N-R, which links the large and the small domains (PLP and Asn194 in the large domain and Arg386 in the small domain), additional mutations easily altered the domain interaction. The R386L mutation on N194A AspAT resulted in the outward movement of the small domain (Figure 4). The Cγ and Cδ atoms of Arg386 are 3.6−3.9 Å from Cβ of Pro195, and a van der Waals interaction seems to exist between the two side chains. Pro195 is located in the large domain and Arg386 in the small domain. Incorporation of a methyl group at Cγ by R386L mutation would reduce the van der Waals interaction between Pro195 and Leu386, and therefore, is most probably the cause of the movement of the small domain. Due to this movement, the ionic interaction between the carboxylate group of Asp15, which is located in the small domain, and the guanidinium group of Arg292*, which is located in the large domain, is weakened. The distance between Cγ of Asp15 and Cζ of Arg292* is 4.0 Å in the wild-type and N194A/Y225F AspAT, whereas the value is 5.9 Å in N194A/R386L AspAT. This, in turn, suggests that the outward movement of the small domain would be made easier if the ionic interaction between Asp15 and Arg292* is lost by mutation of Arg292*. Consistent with this, comparison of the crystal structures of N194A/Y225F and N194A/R292L AspATs showed that the small domain of N194A/R292L AspAT moved outward, whereas N194A/Y225F AspAT maintained the conformation of the wild-type enzyme (Figure 5).[6]

Effect of R292L Mutation on the PLP−Asn194−Arg386 Linkage. From the above discussions, it is expected that the strain of the Schiff base provided by PLP-N-R is increased by R292L mutation. To test this, mutations involving Asn194 and Arg386 were analyzed on R292L AspAT. The R386L mutation on N194A/R292L AspAT showed a ΔpK_a value of 0.12. Thus, the electrostatic effect of Arg386 on the Schiff base does not change much between the Arg292 series and the Leu292 series enzymes (0.12 each). The removal of PLP-N-R by the N194A mutation on R292L AspAT and the wild-type AspAT caused ΔpK_a = 2.09 and 1.68, respectively. This indicates that the R292L mutation actually increased the PLP-N-R-mediated strain of the Schiff base, to yield 0.41 decrease in the Schiff base pK_a.

Electrostatic Effect of Arg292 and Arg386 on the Schiff Base.* The results presented above have indicated that mutations of Arg292* and/or Arg386 alter PLP-N-R and

[4] Assuming that the relative dielectric constant between Arg386 and the Schiff base is not changed by the N194A mutation, the electrostatic contribution of the positive charge of Arg386 to lowering the Schiff base pK_a is calculated to be 0.14, corrected for the change in the distance between Cζ of Arg386 and the imine N by the N194A mutation. However, the change brought about by the correction is so small that it does not essentially alter the discussion.

[5] The value of ΔpK_a = 1.68 for the N194A mutation was still less than ΔpK_a = 2.8, which is brought about by complete relaxation of the Schiff base (*12*). We consider that this is due to the incomplete relaxation of the Schiff base of N194A AspAT. That is, even if Asn194 is removed, a hydrogen bond still remains between O3′ and the phenolic hydroxyl group of Tyr225, and there is a van der Waals contact between the pyridine ring and Ala224. These structures prevent the free rotation of the pyridine ring (*12*).

[6] The backbone conformation of N194A/R292L/R386L AspAT was more close to those of N194A/R292L and N194A/R386L AspATs (RMS < 0.29 Å) than that of the wild-type AspAT (RMS = 0.50 Å), again consistent with this notion.

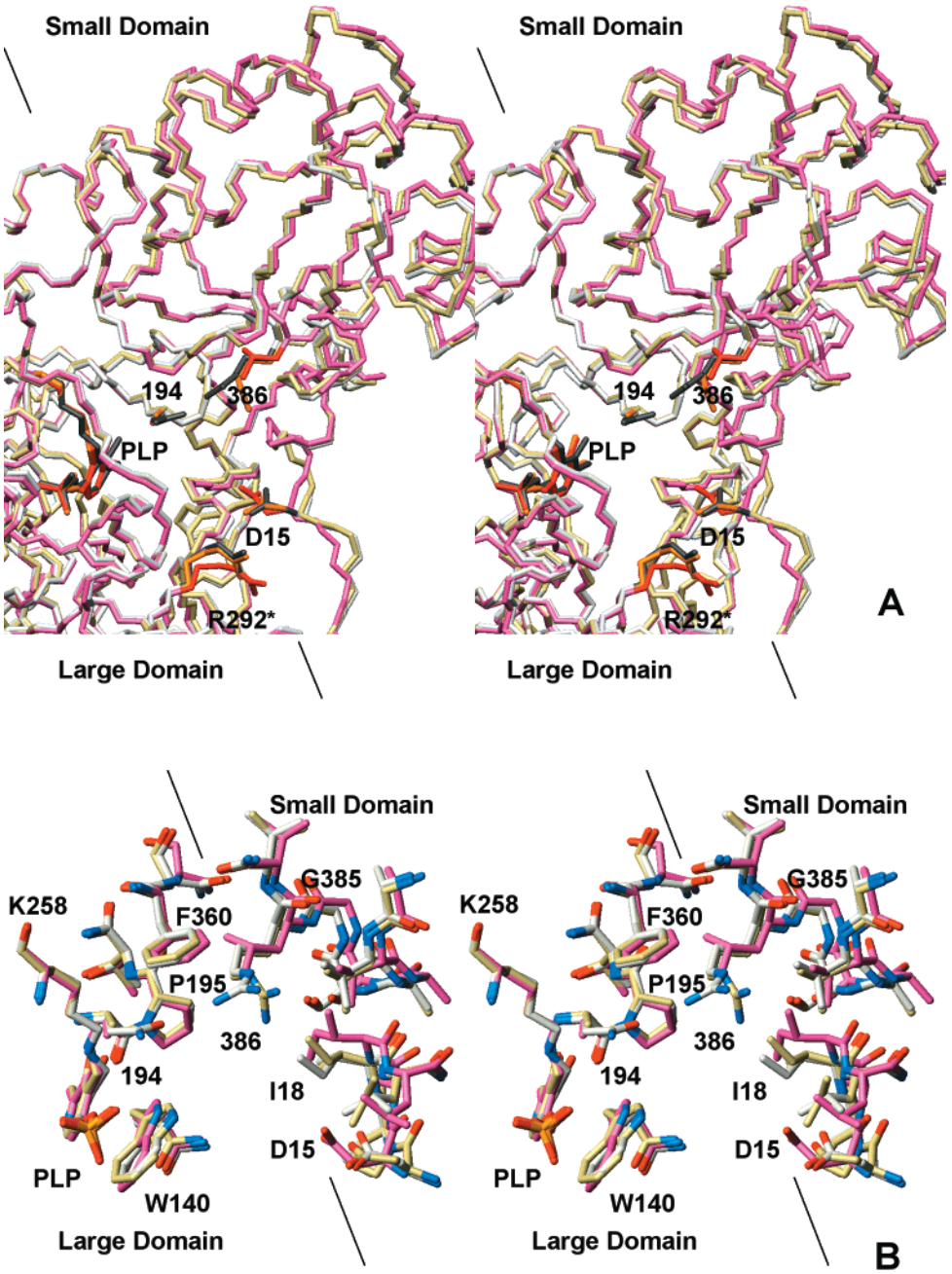

FIGURE 4: (A) Stereodrawing of superimposed structures of the main chains of the wild-type (light gray), N194A/Y225F (khaki), and N194A/R386L (pink) AspATs. The side chains of Lys258 (with PLP), Asp15, Arg292*, and of the residues 194 and 386 are shown in dark colors. Lines show the interface of the large and small domains. (B) Enlargement of the active site showing the relationship of the residues Pro195 and Arg386 or Leu386.

obscure the evaluation of the electrostatic interactions of the individual residues with the Schiff base. Therefore, the electrostatic effects of the two arginine residues are better analyzed in the series of N194A mutant enzymes. For this series, ΔpK_a values of the R292L and R386L mutations were 0.55 and 0.12, respectively, and ΔpK_a of the R292L/R386L mutation was 0.67. Thus, there was a strict additivity of the mutational effects of Arg292* and Arg386 on the Schiff base pK_a, if PLP-N-R had been broken in advance by N194A mutation. This allows us to consider that the ΔpK_a values obtained by the mutation of Arg292* and/or Arg386 on the N194A enzyme reflect the *pure* electrostatic effect of these arginine residues on the Schiff base.

That Arg292* has a more dominant electrostatic effect on the Schiff base than Arg386 was an unexpected finding, because Cζ of Arg292* is more distant (14.5 Å) from the imine N of the Schiff base than Cζ of Arg386 (9.8 Å) in the wild-type AspAT. A difference in the dielectric constant around the arginine residues may explain the discrepancy. However, the precise molecular mechanism for this is not clear at present.

Evaluation of the Mutational Analysis. Several points should be addressed before interpreting the results of the mutational analysis described above. Conformational change of the enzyme protein upon mutation leads to both changes in position of the charged side chains and rearrangement of the hydrogen bond network. Although the conformational changes of AspAT on the mutations described above were not drastic, it is important to know how much these conformational changes alter the electrostatic potential around

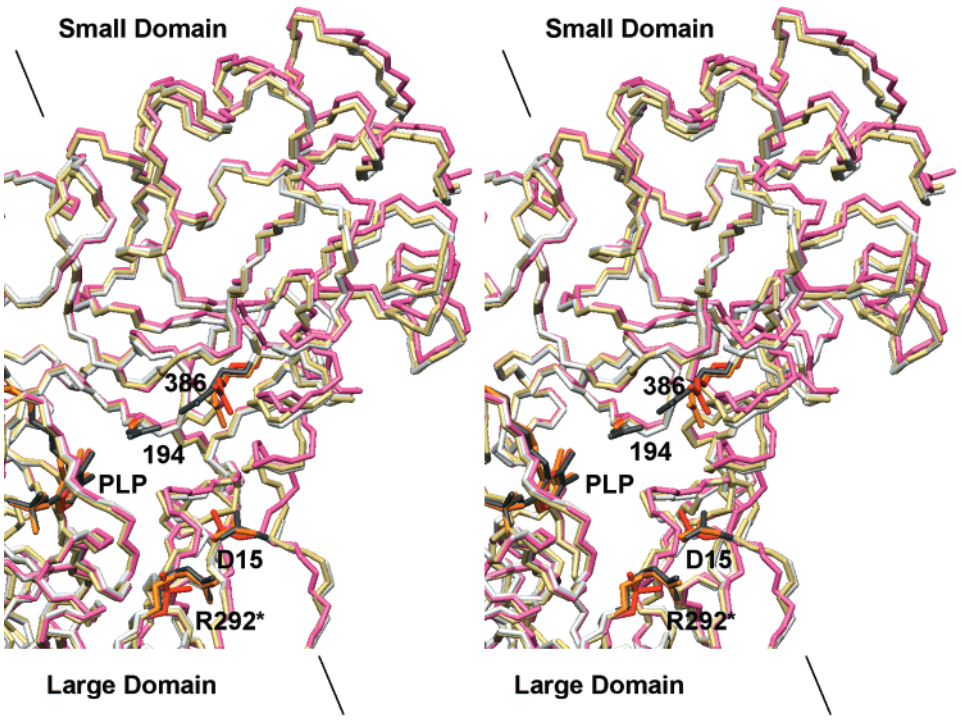

FIGURE 5: Stereodrawing of superimposed structures of the main chains of the wild-type (light gray), N194A/Y225F (khaki), and N194A/R292L (pink) AspATs. The side chains of Lys258 (with PLP), Asp15, Arg386, and of the residues 194 and 292* are shown in dark colors. Lines show the interface of the large and small domains.

the Schiff base. Therefore, using a simple electrostatic model we roughly estimated the total electrostatic interaction energy between the charged groups and the Schiff base N (see Experimental Procedures). The differences in the interaction energy (mutant minus the wild-type) were −0.34 (N194A/R292L), +0.9 (N194A/R386L), and +0.003 kJ mol^{-1} (N194A/R292L/R386L). On the basis of eq 4, the differences in the interaction energy are considered to shift the Schiff base pK_a values by +0.06 (N194A/R292L) and −0.16 (N194A/R386L) and have no apparent effect on the pK_a value of N194A/R292L/R386L. This suggests that the values of the electrostatic effects of Arg292* and Arg386, and the structural effect of PLP-N-R on the Schiff base pK_a, obtained as above, may vary up to 0.16 pH unit. However, we must keep in mind that the electrostatic calculations described above use a simplified model, and advanced calculations may yield larger values of the change in the electrostatic effects of the charged groups. Thus, the above calculations suggest our estimations on the individual contribution of Arg292*, Arg386, and PLP-N-R are qualitatively correct, but cannot rigorously rule out the perturbations by the conformational changes upon mutations.

In addition to Asn194, the phenolic hydroxyl group of Tyr225 forms a hydrogen bond with O3′ of PLP. The presence of Tyr225 has been shown to decrease the Schiff base pK_a value by 1.6 (*19*). Therefore, a change in strength of this hydrogen bond will affect the Schiff base pK_a. The crystal structures of N194A/R292L, N194A/R386L, and N194A/R292L/R386L showed that the Tyr225 side chains of the three mutants are superimposable, and the distance between the phenolic O and O3′ of PLP is increased by 0.3 Å compared with the wild-type AspAT. This is a consequence of the movement of O3′ toward the *si* face of the Schiff base, which is caused by the relaxation of the Schiff base. Although the crystal structure of N194A and other mutant enzymes are not known, the structural data available at present suggest that the value of the effect of N194A mutation described above may include the contribution of the weakening of the O3′−Tyr225 hydrogen bond. This contribution is canceled out when we compare the series of N194A mutant enzymes and deduce the electrostatic effect of the two arginine residues, and when we apply N194A mutation to both the wild-type and R292L enzymes to assess how much R292L mutation increases the strain of PLP-N-R. However, the contribution is contained in the value of 1.68 for the Schiff-base-pK_a-lowering effect of PLP-N-R, and the value of 0.34 for the "PLP-N-R-mediated effect" of R386L mutation, because we compared the Asn194 and Ala194 enzymes to obtain these values.

Increase in the Schiff Base pK_a Value by Dicarboxylic Ligands. The binding of the dicarboxylic substrate analogue maleate increases the pK_a value of the internal aldimine by 2 (*20*). This increase in the pK_a has been explained historically by the neutralization of the positive charges of the two arginine residues (*21*). The present results showed

[7] The O3′-Tyr225 hydrogen bond is considered to decrease the Schiff base pK_a by (1) maintaining the distorted conformation of the Schiff base in the same way as Asn194 (*12*) or by (2) preventing the negative charge of O3′ from entering into the Schiff base (*19*). According to mechanism 1, the maleate-induced increase in the Schiff base pK_a (ΔpK_a) is calculated from the energies gained by conformational relaxation of the Schiff base and by neutralization of the arginine residues, and the increase in length of the O3′-Tyr225 hydrogen bond (0.3 Å) on binding of maleate to the enzyme (*7*) is not considered to be involved in the pK_a increase. On the other hand, according to mechanism 2, the increase in length of the O3′-Tyr225 hydrogen bond destabilizes the negative charge of O3′, and increases further the Schiff base pK_a. The extent of the pK_a increase by this factor is difficult to estimate. However, the close agreement of the observed ΔpK_a value and the estimated ΔpK_a value based on mechanism 1 suggests that the contribution of the factor that originates from mechanism 2 is not significant.

that the positive charges of the two arginine residues decrease the pK_a only by 0.67. Therefore, the electrostatic mechanism can only partially explain the upward shift in the Schiff base pK_a on maleate binding.

We have previously demonstrated that the strain of the protonated PLP−Lys258 Schiff base, which is maintained by Lys258, Ala224, PLP-N-R, and possibly Tyr225, decreases the Schiff base pK_a by 2.8 (*12*). This shows that the strain rather than the electrostatic effect of the two arginine residues is more important in controlling the Schiff base pK_a in the unliganded enzyme, and suggests that the shift in the Schiff base pK_a on binding of maleate should be discussed based on the combination of "strain" and "electrostatic" mechanism.

In the unliganded AspAT, the torsion angle around C4−C4′ (χ) of the protonated Schiff base is 35° (*5*). Binding of maleate to AspAT induces the conformational change in the enzyme from the open form to the closed form (*7*). During the change, the small domain approaches the large domain and relaxes PLP-N-R, thereby decreasing the C4−C4′ torsion angle of the Schiff base (protonated form) from 35° to 25° (*7*). The MOPAC calculation showed that the energy level of the Schiff base is decreased by 7.4 kJ mol^{-1} by this change in the torsion angle (*12*). This corresponds to a 1.3 unit increase in the pK_a value. Therefore, in combination with the neutralization of the two arginine residues, the increase in the Schiff base pK_a on binding of maleate to AspAT is estimated to be 1.97 (1.3 + 0.67). This is in excellent agreement with the observed value of 2.0.[7]

The present study indicates that, contrary to the classical explanation, a relatively small part of the increase in pK_a on binding of ligands to AspAT is caused by neutralization of the positive charges of Arg292* and Arg386. The rest is considered to be due to the conformational change in the Schiff base. This change is caused by the interaction of Arg386 with the α-carboxylate group and is mediated by PLP-N-R. Therefore, we can say that Arg386 is responsible for 1.42 (1.3 + 0.12; the sum of the conformational and electrostatic effects) out of the 2.0-unit increase in the pK_a.

The AspAT superfamily includes the aminotransferases for aspartate, aromatic amino acids, alanine, and histidinol phosphate. Except for AspAT, these aminotransferases use neutral amino acids as substrates, in addition to glutamate (α-ketoglutarate). Therefore, the historical mechanism, in which neutralization of the positive charge of the substrate-binding arginine residues increases the pK_a of the Schiff base (*21*), cannot be directly applied to these enzymes, because neutral amino acids cannot neutralize the positive charge of Arg292*, the residue that binds the ω-carboxylate group of dicarboxylic substrates. The findings of this study, together with the recent finding that the torsion of the Schiff base is the critical factor for decreasing the Schiff base pK_a (*12*), suggest that the interaction of Arg386 and the α-carboxylate group of substrates is the main factor in the increase in the Schiff base pK_a on ligand binding in AspAT. All amino acids have the α-carboxylate group; therefore, the mechanism involving the interaction of α-carboxylate and Arg386 can be applied to the aminotransferases that act on neutral amino acids. In this respect, it is important to perform similar analyses on other aminotransferases of the AspAT family. The work is now under way in this laboratory.

REFERENCES

1. Ovchinnikov, Y., Egorov, C. A., Aldanova, N. A., Feigina, M. Yu., Lipkin, V. M., Abdulaev, N. G., Grishin, E. V., Kiselev, A. P., Modyanov, N. N., Braunstein, A. E., Polyanovsky, O. L., and Nosikov, V. V. (1973) *FEBS Lett. 29*, 31−34.
2. Kirsch, J. F., Eichele, G., Ford, G. C., Vincent, M. G., Jansonius, J. N., Gehring, H., and Christen, P. (1984) *J. Mol. Biol. 174*, 497−525.
3. Kiick, D. M., and Cook, P. F. (1983) *Biochemistry 22*, 375−382.
4. Arnone, A., Rogers, P. H., Hyde, C. C., Briley, P. D., Metzler, C. M., and Metzler, D. E. (1985) in *Transaminases* (Christen, P., and Metzler, D. E., Eds.) pp 138−154, John Wiley & Sons, New York.
5. Rhee, S., Silva, M. M., Hyde, C. C., Rogers, P. H., Metzler, C. M., Metzler, D. E., and Arnone, A. (1997) *J. Biol. Chem. 272*, 17293−17302.
6. McPhalen, C. A., Vincent, M. G., and Jansonius, J. N. (1992) *J. Mol. Biol. 225*, 495−517.
7. Jäger, J., Moser, M., Sauder, U., and Jansonius, J. N. (1994) *J. Mol. Biol. 239*, 285−305.
8. Okamoto, A., Higuchi, T., Hirotsu, K., Kuramitsu, S., and Kagamiyama, H. (1994) *J. Biochem. 116*, 95−107.
9. Toney, M. D., and Kirsch, J. F. (1993) *Biochemistry 32*, 1471−1479.
10. Gloss, L. M., and Kirsch, J. F. (1995) *Biochemistry 34*, 3990−3998.
11. Hayashi, H., and Kagamiyama, H. (1997) *Biochemistry 36*, 13558−13569.
12. Hayashi, H., Mizuguchi, H., and Kagamiyama, H. (1998) *Biochemistry 37*, 15076−15085.
13. Inoue, Y., Kuramitsu, S., Inoue, K., Kagamiyama, H., Hiromi, K., Tanase, S., and Morino, Y. (1989) *J. Biol. Chem. 264*, 9673−9681.
14. Cronin, C. N., and Kirsch, J. F. (1988) *Biochemistry 27*, 4572−4579.
15. Hayashi, H., Kuramitsu, S., Inoue, Y., Morino, Y., and Kagamiyama, H. (1989) *Biochem. Biophys. Res. Commun. 159*, 337−342.
16. Kallen, R. G., Korpela, T., Martell, A. E., Matsushima, Y., Metzler, C. M., Metzler, D. E., Morozov, Yu, V., Ralston, I. M., Savin, F. A., Torchinsky, Yu., M., and Ueno, H. (1985) in *Transaminases* (Christen, P., and Metzler, D. E., Eds.) pp 37−108, John Wiley & Sons, New York.
17. Jenkins, W. T., and D'Ari, L. (1966) *J. Biol. Chem. 241*, 5667−5674.
18. Slebe, J. C., and Martinez-Carrion, M. (1976) *J. Biol. Chem. 251*, 5663−5669.
19. Goldberg, J. M., Swanson, R. V., Goodman, H. S., and Kirsch, J. F. (1991) *Biochemistry 30*, 305−312.
20. Yano, T., Mizuno, T., and Kagamiyama, H. (1993) *Biochemistry 32*, 1810−1815.
21. Ivanov, V. I., and Karpeisky, M. Y. (1969) *Adv. Enzymol. Relat. Areas Mol. Biol. 32*, 21−53.
22. Kuramitsu, S., Hiromi, K., Hayashi, H., Morino, Y., and Kagamiyama, H. (1990) *Biochemistry 29*, 5469−5476.
23. Sakabe, N. (1991) *Nucl. Instrum. Methods Phys. Res. A303*, 448−463.
24. Higashi, T. (1989) *J. Appl. Crystallogr. 22*, 9−18.
25. Brunger, A. T., Kuriyan, K., and Karplus, M. (1987) *Science 235*, 458−461.
26. Cambiilau, C., and Horjales, E. (1987) *J. Mol. Graphics 5*, 174−177.
27. Laskowski, R. A., MacArthur, M. W., Moss, D. S., and Thornton, J. M. (1993) *J. Appl. Crystallogr. 26*, 283−291.
28. Gelin, B. R., and Karplus, M. (1979) *Biochemistry 18*, 1256−1268.
29. Danishefsky, A. T., Onnufer, J. J., Petsko, G. A., and Ringe, D. (1991) *Biochemistry 30*, 1980−1985.
30. Koradi, R., Billeter, M., and Wüthrich, K. (1996) *J. Mol. Graphics 14*, 51−55.

BI001403E